Molecular Biology of the Cell
Vol. 11, 1011–1022, March 2000

Discontinuous Actin Hexagon, a Protein Essential for Cortical Furrow Formation in *Drosophila*, Is Membrane Associated and Hyperphosphorylated

Claire X. Zhang,* Wendy F. Rothwell,† William Sullivan,† and Tao-shih Hsieh*‡

*Department of Biochemistry, Duke University Medical Center, Durham, North Carolina 27710; and †Sinsheimer Laboratories, Department of Biology, University of California, Santa Cruz, California 95064

Submitted July 6, 1999; Revised December 7, 1999; Accepted December 21, 1999
Monitoring Editor: John C. Gerhart

discontinuous actin hexagon (*dah*) is a maternal-effect gene essential for the formation of cortical furrows during *Drosophila* embryogenesis, and DAH protein colocalizes with actin in these furrows. Biochemical fractionation experiments presented here demonstrate that DAH is highly enriched in the membrane fraction and that its membrane association is resistant to high-salt and alkaline washes. Furthermore, it partitions into the detergent phase of the Triton X-114 solution, indicating its tight binding to the membranes. DAH can also interact with the actin cytoskeleton, because a fraction of DAH remains insoluble to nonionic detergent along with actin. These biochemical characterizations suggest that DAH may play a role in the linkage of the actin cytoskeleton to membranes. Using phosphatase inhibitors, we detected multiple phosphorylated forms of DAH in embryonic extracts. The DAH phosphorylation peaks during cellularization, a stage at which DAH function is critical. A kinase activity is coimmunoprecipitated with the DAH complex and hyperphosphorylates DAH in vitro. Purified casein kinase I can also hyperphosphorylate DAH in the immune complex. Both DAH localization and phosphorylation are disrupted in another maternal-effect mutant, *nuclear-fallout*. It is possible that *nuclear-fallout* collaborates with *dah* and directs DAH protein localization to the cortical furrows.

INTRODUCTION

Drosophila early embryogenesis is characterized by 13 rapid nuclear divisions in a syncytium (Rabinowitz, 1941; Foe and Alberts, 1983). The first 9 nuclear divisions occur in the interior of the embryo. By the interphase of cycle 10, the majority of nuclei reach the cortex and undergo 4 more synchronous divisions as an evenly spaced monolayer underneath the plasma membrane. These 4 nuclear divisions, cycles 10–13, are termed the syncytial blastoderm stage. Cellularization occurs during the interphase of cycle 14; the plasma membrane invaginates ~6000 cortical nuclei to form individual cells. The highly ordered developmental events are largely dependent on the cytoskeletal organizations (reviewed by Fyrberg and Goldstein, 1990; Schejter and Wieschaus, 1993). During the syncytial blastoderm, the actin cytoskeleton undergoes rearrangements in each nuclear division, forming caps above the interphase nuclei and moving into the transient metaphase furrows when mitosis starts (Karr and Alberts, 1986; Kellogg *et al.*, 1988). At the interphase of cycle 14, the actin cytoskeleton is associated with the invaginating membranes, especially in the furrow canals at the membrane front. The cleavage furrows proceed almost synchronously to cellularize ~6000 nuclei within a period of ~45 min.

Although the cytoskeleton dynamics has been well characterized, it remains unsolved how these networks are organized and controlled during development. Genetic analysis has revealed several maternal-effect genes required for the early cortical organizations. *daughterless-abo-like*, *sponge*, and *scrambled* mutants have distinctive defects in the actin networks during the syncytial blastoderm, whereas the cleavage furrows during the cellularization process appear relatively normal (Sullivan *et al.*, 1990, 1993; Postner *et al.*, 1992). *nuclear-fallout* has recently been cloned; it encodes a centrosomal protein critical for both metaphase furrows and cleavage furrows (Rothwell *et al.*, 1998). The NUF protein localizes to the centrosomes during the prophase of syncytial blastoderm and throughout the cellularization process, suggesting a role in setting up the cortical furrows. Cytological analysis also shows early defects in actin recruitment at these stages in the *nuf* mutant (Rothwell *et al.*, 1998). Because

‡ Corresponding author. E-mail address: hsieh@biochem. duke.edu.

the maternal-effect gene *grapes* is a yeast *checkpoint 1* (*chk1*) homologue (Fogarty *et al.*, 1997; Sibon *et al.*, 1997), the cytoskeletal defects in the *grp* mutant are most likely the result of defective cell cycles during the late blastoderm stages. At cycle 14, three zygotic genes, *nullo*, *serendipity-α*, and *bottleneck*, in addition to the maternal genes, are required for the proper progression of cellularization (Merrill *et al.*, 1988; Wieschaus and Sweeton, 1988; reviewed by Schejter and Wieschaus, 1993). It has been proposed that these zygotic genes remodel the cytoskeleton structure for the cellularization process, which was initially set up by the maternal genes (Schejter *et al.*, 1992).

We previously identified a maternal-effect gene, *discontinuous actin hexagon* (*dah*), which is required for cortical furrow formation (Zhang *et al.*, 1996). The DAH protein is mainly found in 0- to 6-h embryos, and the protein expression reaches its peak around the cellularization stage. It localizes to the metaphase furrows at the syncytial blastoderm and to the cleavage furrows during cellularization. It also shows a particulate staining pattern in the cell cortex where phosphotyrosyl proteins are colocalized, suggesting that they are membrane vesicles (Rothwell *et al.*, 1999). These DAH particles are recruited to the furrow structures and participate in membrane invagination. The null mutant of *dah* shows defective metaphase furrows. These furrows are discontinuous and, moreover, they fail to extend. It is possible that DAH is involved in recruiting critical furrow components, such as lipids and the actin cytoskeleton, to the furrows. The cleavage furrows in cellularizing mutant are totally disorganized, possibly as a result of the high demand of membrane synthesis. All these data indicate that DAH is directly involved in cortical furrow formation. The DAH protein sequence reveals a modest but statistically significant homology to the dystrobrevins and the carboxyl-terminal domains of dystrophin. Therefore, DAH may play a role similar to that of dystrophin in anchoring the actin cytoskeleton to membranes, and this linkage is crucial for furrow formation.

In this paper, we present a biochemical analysis demonstrating that DAH is tightly associated with membrane and is hyperphosphorylated during furrow formation. To understand the regulation of *dah* during fly development, we explore the possibility of *dah* interacting with other maternal-effect genes by monitoring the expression, phosphorylation, and localization of DAH in these mutants.

MATERIALS AND METHODS

Cell Fractionation and Treatment of Membrane Fractions with Solubilizing Agents

Fractionation of embryonic extracts was performed according to Strand *et al.* (1994) with the following modifications. One gram of 0- to 4-h embryos was homogenized in 3 ml of buffer H (50 mM Tris-HCl, pH 7.5, 150 mM KCl, 5 mM $MgCl_2$, 0.25 M sucrose, 0.1 mM DTT, 1 mM PMSF, 2 μg/ml leupeptin, 2 μg/ml pepstatin) and filtered through two layers of 120-μm Nitex screen. The filtrate was loaded on a 0.5/2/2.5 M sucrose step gradient in a Beckman (Fullerton, CA) SW27 rotor centrifuge tube. After centrifugation at 24,000 rpm for 2.5 h, the membrane fraction, cytosolic fraction, and nuclear pellet were recovered. The membrane fraction was diluted in 2 volumes of buffer H and sedimented at 30,000 × *g* for 20 min. The membrane pellet was resuspended in 10 ml of buffer H and sedimented again. The cytosolic fraction was also further purified by diluting it in 7 volumes of buffer H and centrifuged. The nuclear pellet was washed in 10 ml of buffer H and sedimented at 1000 × *g* for 15 min. The identity and purity of the cellular fractions were monitored as follows. Individual nuclei in the nuclear fraction were identified by DAPI (Sigma Chemical, St. Louis, MO) staining. Almost 100% of the GAPDH activity in the cell was found in the cytosolic fraction, whereas <10% of the activity was found in the nuclear and membrane fractions. GAPDH activity was assayed according to McAlister and Holland (1985). Membrane vesicles of different sizes were observed only in the membrane fraction by light microscopy. Furthermore, we also found two *Drosophila* membrane proteins, neurexin and coracle (Baumgartner *et al.*, 1996; Ward *et al.*, 1998), in our membrane preparations.

The membrane pellet was resuspended in 200 μl of buffer H and divided into aliquots and placed in five tubes for treatment with solubilizing agents. The aliquots were incubated with 1 ml of PBS, 1 M KI (freshly made in 50 mM Tris-HCl, pH 7.5), 100 mM Na_2CO_3 (pH 10), 100 mM glycine (pH 2.8), and 1% NP-40 (in 50 mM Tris-HCl, pH 7.5), respectively, for 30 min at room temperature. The suspensions were centrifuged at 30,000 × *g* for 20 min. The pellets were solubilized in SDS sample buffer, and the supernatants were precipitated in trichloroacetic acid, followed by solubilization in SDS sample buffer. Western blot analysis was carried out as described previously (Zhang *et al.*, 1996).

For detergent extraction, membranes prepared from 0.5 g of embryos were resuspended in 0.5 ml of 1% NP-40 or 1% SDS. The NP-40 suspension was incubated on ice for 10 min and centrifuged at 30,000 × *g* for 20 min. The supernatant was saved, and the pellet was extracted three more times with 1% NP-40. The final pellet was resuspended in SDS sample buffer directly. The SDS suspension was incubated at room temperature for 30 min and centrifuged. The supernatant was saved, and the pellet was extracted one more time.

Triton X-114 Phase Separation

The membrane pellet prepared from the sucrose density gradient sedimentation was resuspended in 250 μl of 1% Triton X-114 solution, followed by the phase separation, which was performed according to Bordier (1981). The Triton X-114 phase separation has also been carried out with total embryonic extracts. Staged embryos were homogenized 1:10 (wt/vol) in buffer with 10 mM Tris-HCl, pH 7.4, 150 mM NaCl, 1% Triton X-114, 1 mM DTT, 10 μg/ml leupeptin, 10 μg/ml pepstatin, and centrifuged at 600 × *g* for 10 min. The supernatant then underwent Triton X-114 phase separation.

Phosphatase Inhibitors and λ Protein Phosphatase Treatment

One of the protein phosphatase inhibitors, 1 mM Na_3VO_4, 60 mM NaF, 1 μM okadaic acid (Sigma Chemical), and 1 μM microcystin-LR (Sigma Chemical) was included in the homogenization buffer when protein extractions were performed according to Lee *et al.* (1993). As controls, embryos were lysed either in SDS sample buffer or first in homogenization buffer followed by the addition of sample buffer. Treatment of the extracts with λ protein phosphatase (New England Biolabs, Beverly, MA) was performed according to the manufacturer's protocol.

Single-Embryo Western Blot

Embryos from 0- to 2-h collections were dechorionated as described previously (Zhang *et al.*, 1996). They were transferred to slides, immersed in halocarbon oil 700 (Halocarbon Laboratories, Hackensack, NJ), and observed under a light microscope (Laborlux, E. Leitz, Rockleigh, NJ). Each embryo was staged by its morphology and nuclear density, disrupted, and transferred into SDS sample buffer for Western blot analysis.

Immunoprecipitation and Kinase Assays

Staged embryos (0.05 g) were lysed in 1.5 ml of buffer N (50 mM Tris-HCl, pH 8, 150 mM NaCl, 1% NP-40, 1 mM PMSF, 1 mM DTT, 2 μg/ml leupeptin, 2 μg/ml pepstatin) and centrifuged at 10,000 $\times$ *g* for 20 min. The supernatant was incubated with antibody-coupled protein A beads for 2 h at 4°C. To prepare antibody-coupled protein A beads, 3 μl of affinity-purified antibody was added to 100 μl of buffer N and incubated with 10 μl of protein A beads (Sigma Chemical) for 0.5 h at 4°C. The beads were then sedimented by a quick spin and washed twice with 1 ml of buffer N before they were ready for use. After the incubation with the embryonic extract, the beads were sedimented and washed four times with buffer N or other wash solutions and two times with 20 mM Tris-HCl. Then they were incubated with 30 μl of kinase reaction buffer containing 20 mM Tris-HCl, pH 8, 10 mM $MgCl_2$, 1 mM DTT, and 1 mM [γ-^{32}P]ATP (300 Ci/mmol) for 1 h at room temperature. For exogenous kinase reactions, 5–20 U of purified kinases, casein kinase I, $p34^{cdc2}$/cyclin B protein kinase, casein kinase II, catalytic subunit of cAMP-dependent protein kinase, MAPK (Erk2), and glycogen synthase kinase 3, all of which were purchased from New England Biolabs, and the catalytic domain of PKC, which was generously provided by Drs. Y. Shi and P. Blackshear (Graff *et al.*, 1991), were applied in a 30-μl reaction mixture. The kinase assays were performed for 1 h according to the manufacturer's procedure or Graff *et al.* (1991). The kinase reactions were stopped by washing the beads with 1 ml of 20 mM Tris-HCl, pH 8, and adding the SDS sample buffer. The samples were then subjected to gel electrophoresis, silver staining according to the manufacturer's protocol for the Silver Stain Plus kit (Bio-Rad Laboratories, Hercules, CA), and autoradiography.

Fly Stocks

Female-sterile mutants *sced*, *spg*^{335}, and *dal*^{1} were generously provided by the laboratories of W. Theurkauf (State University of New York, Stony Brook, NY), C. Nuesslein-Volhard (Max Planck Institute for Developmental Biology, Tübingen, Germany), and the Bloomington *Drosophila* Stock Center (Bloomington, IN), respectively. *nuf*, *grp*^{1034}, and *wdel* mutants were from W. Sullivan's laboratory stocks. *dah*^{30} mutant was from T.-s. Hsieh's laboratory stock.

Immunofluorescence Staining of Whole-Mount Embryos

Embryos of 1- to 3-h collections from the wild type and various homozygous female-sterile mutant mothers were prepared for immunofluorescence microscopy as described (Zhang *et al.*, 1996). The laser scanning confocal images were collected with the use of a fluorescence microscope (Axiovert, Carl Zeiss, Thornwood, NY) equipped with a 40X/1.2 Plan-Neofluar lens.

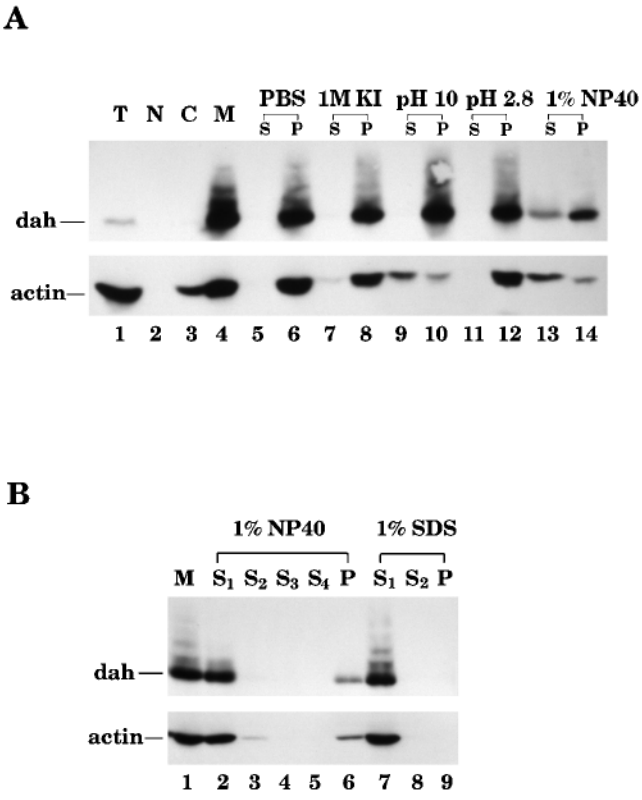

Figure 1. DAH is tightly associated with membranes. (A) Embryos (0–4 h) were prepared for cellular fractionation on a sucrose step gradient. Total extract (T) and nuclear (N), cytosolic (C), and membrane (M) fractions were loaded on a SDS 8% polyacrylamide gel and subjected to Western blot analysis by DAH and actin antibodies. Twenty-five micrograms of total proteins was loaded in lanes 1, 2, and 4, and 12 μg was loaded in lane 3. DAH protein is concentrated in the membrane fraction (lane 4). Various solubilizing reagents were used to wash the membranes prepared from the fractionation experiment. These reagents were PBS, 1 M KI, 100 mM Na_2CO_3 (pH 10), 100 mM glycine (pH 2.8), and 1% NP-40. After washing, the same volume of supernatant (S) and pellet (P) was loaded on the gel and subjected to Western blot analysis. DAH protein can be solubilized only from the membrane by 1% NP-40 (lane 13). (B) The membrane fractions (M) underwent four washes in 1% NP-40 or two washes in 1% SDS. Equal volumes of the supernatants (S_1, S_2, S_3, and S_4) from each wash and the final pellet (P) were loaded onto a gel for Western blot analysis. A fraction of DAH remains insoluble in the nonionic detergent NP-40 (lane 6).

RESULTS

DAH Is Tightly Associated with Membranes

Our previous study showed that DAH localizes to cortical furrows and to particles where phosphotyrosyl proteins are also colocalized, suggesting that they may be membrane vesicles (Zhang *et al.*, 1996; Rothwell *et al.*, 1999). The crucial roles of DAH in furrow formation suggest that DAH may exert its function in the membranes. To test if DAH is mainly membrane associated, we performed cellular fractionation experiments with early embryos. Nuclear, cytosolic, and membrane fractions were isolated according to their buoyant densities in sucrose step gradients. The purity of these fractions was monitored (see MATERIALS AND METHODS). Western blot analysis revealed that the DAH protein is highly enriched in the membrane fraction but absent in the nuclear and cytosolic fractions (Figure 1A, lanes 1–4). Actin is also found in the membrane fraction, consistent with its role in the cortical furrows (Figure 1A, lower panel, lanes 3 and 4) (Strand *et al.*, 1994). To understand the nature of DAH association with membranes, we treated the membrane fraction with various solubilizing reagents (Figure 1A, lanes 5–14). We used actin as a reference to determine if DAH is associated with membranes through actin networks. DAH remains associated with the membranes after high-salt wash (1 M KI) and acid and alkaline treatments at pH 2.8 and 10, respectively, indicating a tight association between DAH and membrane. In comparison, actin is also resistant to KI

wash and low-pH treatment. However, the majority of actin can be released at high pH, which is characteristic of many peripheral proteins (reviewed by Hortsch, 1994). The different behavior between DAH and actin upon the alkaline treatment suggests that the membrane association of DAH can occur independently of actin networks. It is possible that DAH itself is an integral protein or, alternatively, that it binds tightly to integral proteins in the membrane. As an example of the latter possibility, cytoplasmic protein coracle, which is involved in septate junction formation and associates with membranes through its interaction with the transmembrane protein neurexin (Baumgartner *et al.*, 1996; Ward *et al.*, 1998), was also resistant to the alkaline wash in our membrane preparation (our unpublished results).

Membrane association of DAH was also demonstrated by cloudy point precipitation with Triton X-114, which has been widely used to characterize membrane proteins (Bordier, 1981), including several *Drosophila* proteins (reviewed by Hortsch, 1994). When the cloudy point temperature is reached, Triton X-114 solution separates into a lighter phase of aqueous solution and a detergent-rich lower phase. Integral proteins partition into the detergent phase, whereas most peripheral proteins go into the aqueous phase. The membrane pellet purified from the sucrose gradient was resuspended in Triton X-114 solution, and the phase separation was performed. DAH protein is mainly (>90%) recovered in the detergent phase, whereas ~50% of actin goes into the aqueous phase (Figure 2A, lanes 2 and 3). The detergent fractions of DAH and actin are both stable in repeated Triton X-114 washes (Figure 2A, lanes 4–7). We also treated the total embryonic extract with Triton X-114 to determine if the majority of the DAH population is membrane bound, as the membrane fractionation experiment had suggested. Upon examination of the crude extract, most of the actin is recovered in the aqueous phase, whereas ~60% of DAH is found in the detergent phase (Figure 2B). Partition of DAH between the aqueous and detergent phases does not change in different embryonic stages when 0- to 1-h and 2- to 3-h embryos are compared (Figure 2B). Therefore, the membrane association of DAH is not developmentally regulated.

These biochemical results demonstrate that DAH is tightly associated with membranes. The DAH amino acid sequence reveals no transmembrane domains or signal peptide sequence. However, there are four potential *N*-glycosylation sites in the DAH sequence. To investigate the possibility of glycosylation, we treated DAH protein with peptide:*N*-glycosidase, which cleaves between the innermost *N*-acetylglucosamine and asparagine residues from N-linked glycoproteins (Maley *et al.*, 1989). We did not observe any electrophoretic mobility change of DAH after peptide:*N*-glycosidase digestion (our unpublished results). No consensus sequence for lipid modifications, including myristoylation and farnesylation, are present in the DAH sequence. Because palmitoylation has no defined sequence requirement, it is still possible that DAH may be palmitoylated. We used hydroxylamine treatment on the DAH protein, which can promote the hydrolysis of the thioester bond between the palmitoylate and cysteine (Magee *et al.*, 1984). After extensive treatment of hydroxylamine with membranes prepared from sucrose gradient or membranes from total embryonic extracts prepared by Triton X-114 partition, no difference in DAH electrophoretic mobility was observed (our unpublished results). All these experiments suggest that, rather than being an integral membrane protein, DAH is likely to be associated with membranes through its interactions with other integral proteins. This indirect association of DAH with membranes potentially allows it to play a critical role in reversibly connecting membrane vesicles to other cellular compartments, a function that may be important in the dynamic process of cortical furrow formation.

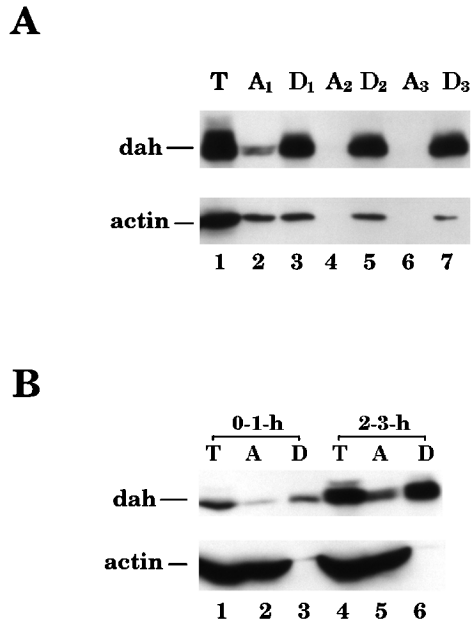

Figure 2. DAH partitions into the Triton X-114 detergent phase. (A) The membrane pellets were resuspended in 1% Triton X-114 solution and subjected to cloudy point precipitation. Equal volumes of the membrane suspension (T), the aqueous phase (A), and the detergent phase (D) were loaded onto a gel for Western blotting. The gel was probed with DAH and actin antibodies. The detergent phase after the first phase separation (D_1) was washed two more times to give rise to A_2 and D_2, and A_3 and D_3, respectively. The majority of the DAH protein in the membrane fraction partitions into the detergent phases (lanes 3, 5, and 7). (B) Crude embryonic extracts (0–1 and 2–3 h) were prepared for Triton X-114 phase separation, and >60% of the DAH protein is in the detergent phase (lanes 3 and 6).

When the nonionic detergent NP-40 was used to solubilize the membranes, we noticed that a fraction of DAH remained insoluble along with actin (Figure 1A, lanes 13 and 14). This has been observed for proteins that interact with the cytoskeleton (Geiger, 1983; Nagafuchi and Takeichi, 1988; Graziani *et al.*, 1989; McCrea and Gumbiner, 1991). We also found that coracle, a component of the septate junctions, is present in the NP-40–insoluble fraction along with actin (our unpublished results). To ensure the complete solubilization of the membranes, we performed serial NP-40 washes. A significant amount of the DAH protein remains in the insoluble aggregates after repeated washes, which parallels the effect on actin (Figure 1B). An ionic detergent, SDS, efficiently solubilizes all the DAH protein and actin. This result suggests that DAH may participate in the actin cytoskeletal matrix, corroborating earlier localization results

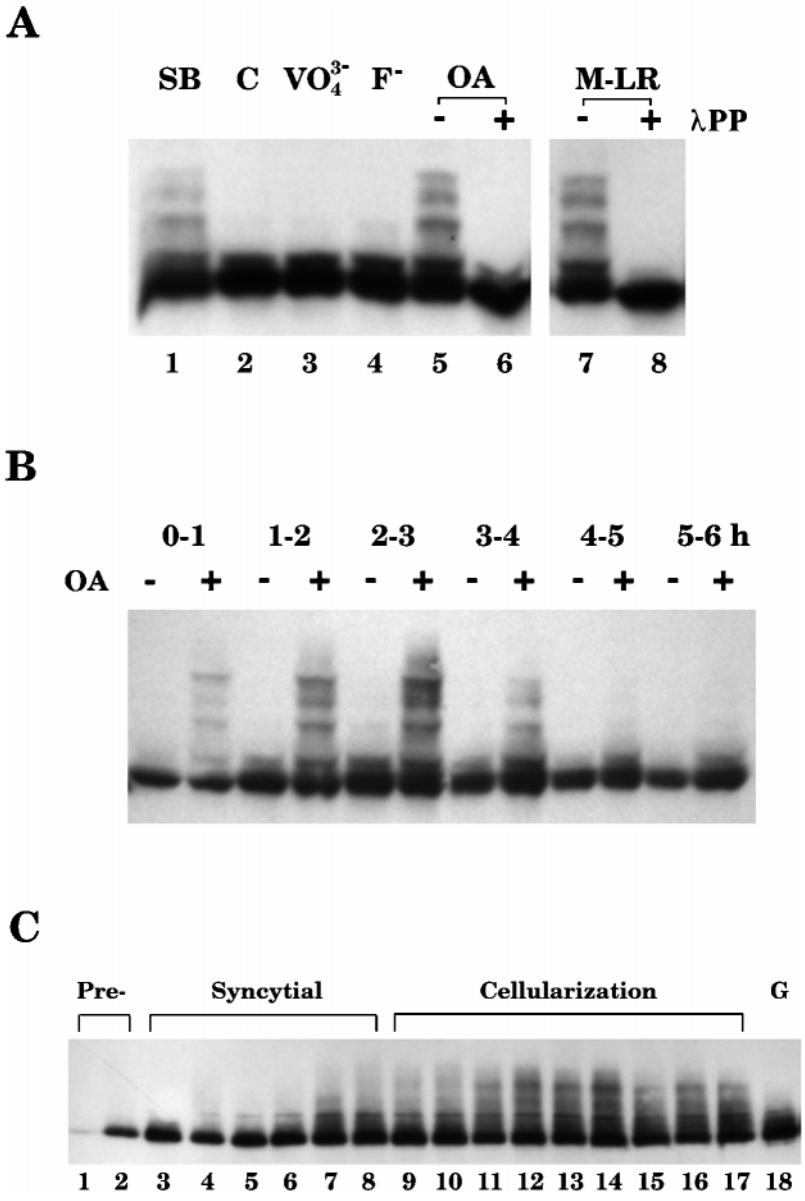

Figure 3. DAH is hyperphosphorylated during cellularization. (A) Different phosphatase inhibitors, VO_4^{3-}, F^-, okadaic acid (OA), and microcystin (M-LR), were included in the homogenization buffer to prepare embryonic extracts. Embryos were also lysed in SDS sample buffer directly (SB) or in homogenization buffer (C). Total proteins (100 μg) were loaded for each sample, and Western blotting with DAH antibody was performed. Several slow-migrating species were detected when OA and M-LR were added (lanes 5 and 7), and they all collapsed to the lowest band after the treatment of λ protein phosphatase (λPP; lanes 6 and 8). (B) Hourly staged embryos during the first 6 h of development were prepared with or without OA for Western blot analysis. DAH phosphorylation reached its peak at 2–3 h. (C) Single embryos were staged according to their morphology and nuclear density by light microscopy. Embryos in the preblastoderm (Pre-), syncytial blastoderm, cellularization, and gastrulation (G) stages were lysed in SDS sample buffer and loaded in the order of development. Embryos in lanes 9 and 10 had not extended their cleavage furrows. Embryos in lanes 11–14 were all in the slow phase of membrane invagination, followed by fast-phase embryos in lanes 15–17. DAH phosphorylation is most extensive during the slow phase of cellularization (lanes 11–14).

by immunofluorescence microscopy (Zhang *et al.*, 1996). However, the interaction between DAH and actin may be indirect. No actin-binding domains can be identified in the protein sequence of DAH. Furthermore, when preexisting actin filaments were cleared from embryonic extracts and actin monomers were polymerized, DAH did not cosediment with the actin filaments (our unpublished results). Similar to its membrane binding, DAH may bind to actin through its interaction with other proteins. This property suggests that DAH could serve as an intermediary in linking membrane vesicles to actin-based cytoskeleton.

DAH Is Hyperphosphorylated during Cellularization

In the immunoblots of DAH, we have detected a minor fraction of DAH protein that migrates at reduced electrophoretic mobilities, suggesting the possibility of posttranslational modifications. We tested whether DAH is phosphorylated in vivo by including phosphatase inhibitors in the homogenization buffer when preparing the embryonic extracts. Vanadate, a tyrosine phosphatase inhibitor, fluoride, a serine/threonine phosphatase inhibitor, and okadaic acid and microcystin, specific for phosphatase I, IIA, and IV, were used. Although vanadate and fluoride had no discernible effect on the distribution of DAH species (Figure 3A, lanes 3 and 4), multiple DAH species with reduced electrophoretic mobilities were recovered when okadaic acid or microcystin was added (Figure 3A, lanes 5 and 7). A similar DAH pattern was found when embryos were lysed directly in SDS sample buffer (Figure 3A, lane 1), confirming that an endogenous phosphatase is responsible for converting the

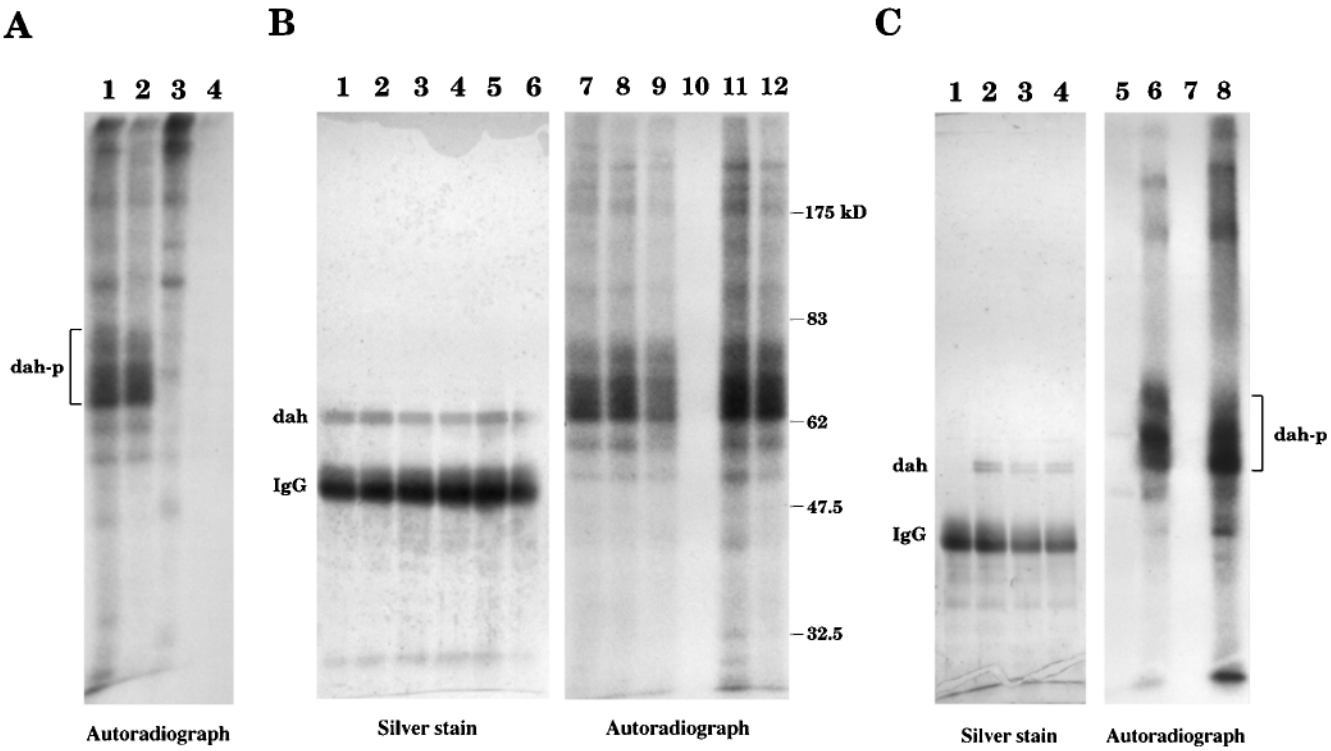

Figure 4. A kinase activity is found in DAH immune complex. (A) Immunoprecipitation with the wild-type 0- to 4-h embryonic extract was carried out by the DAH antibody (lanes 1 and 2) or the preimmune serum (lanes 3 and 4). The immune complex was washed and incubated with [γ-^{32}P]ATP for in vitro kinase assay. Washing with 150 mM NaCl (in buffer N) was used for lanes 1 and 3, and 1 M NaCl was applied for lanes 2 and 4. The samples were loaded onto a gel and subjected to autoradiography. A series of phosphorylated bands were specifically detected in the DAH immunoprecipitates. (B) The DAH immune complex was washed with 150 mM NaCl (lanes 1 and 7), 1 M NaCl (lanes 2 and 8), 4.5 M NaCl (lanes 3 and 9), 1 M KI (lanes 4 and 10), 10 mM EGTA (lanes 5 and 11), and 10 mM EDTA (lanes 6 and 12), all in buffer N, before the kinase reaction. The gel was stained by silver stain (lanes 1–6) and then exposed to a film (lanes 7–12). The kinase activity, but not the DAH protein itself, can be washed off by 1 M KI (lanes 4 and 10). (C) Immunoprecipitation was carried out with the mutant extract (lanes 1 and 5) or the wild-type extract (lanes 2 and 6) before the kinase assay. DAH protein was not detected in the mutant. When the DAH immune complex from the wild-type extract was washed with 1 M KI (lanes 3, 4, 7, and 8), the kinase activity was recovered after the incubation with the mutant extract (lane 8). No activity was observed when the DAH complex was incubated with the homogenization buffer alone (lane 7). dah-p, phosphorylated DAH; IgG, immunoglobulin G.

slow-migrating species into the major fast-migrating species. Addition of an exogenous phosphatase, λ protein phosphatase, can generate results similar to those found with the endogenous phosphatase (Figure 3A, lanes 6 and 8). The single band in lane 8, which migrates slightly faster than the other fast-migrating bands in lanes 1–7, is due to the extensive dephosphorylation reaction of λ protein phosphatase. The fast-migrating species in lanes 1–7 actually consist of two bands, which were resolved on a film with less exposure time (our unpublished results). The DAH band in lane 8 correlates with the lower band of the DAH doublet, which suggests that the upper band is also a phosphorylated species of the DAH protein, and its further phosphorylations result in the multiple slower-migrating bands. The results from the okadaic acid and microcystin treatments indicate that the endogenous phosphatase responsible for DAH dephosphorylation could be phosphatase I, IIA, or IV. These are all serine/threonine phosphatases. In addition, antibody specific for phosphotyrosine fails to recognize any of the DAH phosphorylated species (our unpublished results). Therefore, DAH protein is most likely phosphorylated on serine and threonine residues.

The major interest in DAH phosphorylation lies in its potential regulation of the protein function. To investigate whether DAH phosphorylation is developmentally regulated, different stages of embryos have been examined. The phosphorylation reaches its peak at 2–3 h (Figure 3B), when cellularization occurs. The hyperphosphorylated species were observed only in samples prepared in the presence of a phosphatase inhibitor, okadaic acid. We have quantified the phosphorylated species by densitometric analysis of the Western blot. Up to six phosphorylated species can be clearly counted, and they make up >70% of the total DAH protein at 2–3 h, when DAH expression reaches its peak. In comparison, ~40% of the total DAH protein is phosphorylated in the 0- to 1-h embryos. Because the embryos collected hourly are not synchronous in development, we examined the DAH phosphorylation more precisely in single embryos. Embryos were lysed directly in SDS sample buffer to maintain the hyperphosphorylated state of DAH (Figure 3A, lane

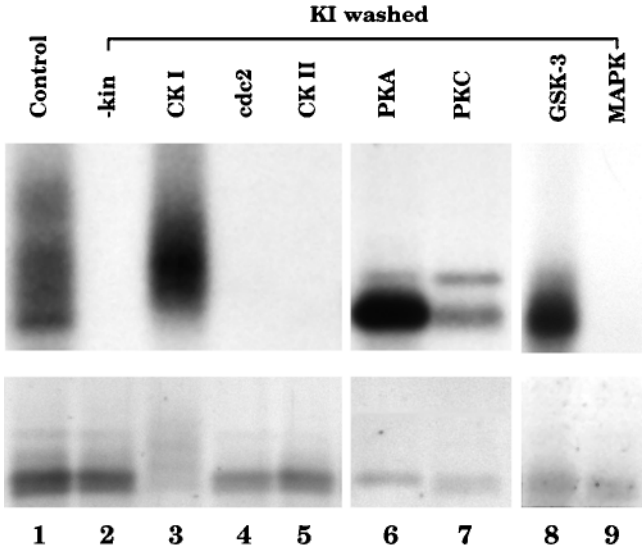

Figure 5. DAH can be hyperphosphorylated by CKI. DAH protein was immunoprecipitated and the endogenous kinase associated with DAH was removed by 1 M KI (lanes 2–9). The DAH immunoprecipitates were then incubated with no kinases (−kin), or with casein kinase I (CK I), $p34^{cdc2}$/cyclin B protein kinase (cdc2), casein kinase II (CK II), cAMP-dependent protein kinase (PKA), PKC, glycogen synthase kinase 3 (GSK-3), and MAPK for kinase reactions (lanes 3–9). These samples were prepared for gel electrophoresis, followed by analysis with silver staining (lower panel) and autoradiography (upper panel). Casein kinase I hyperphosphorylates DAH protein, whereas the other kinases fail to generate a similar phosphorylation pattern as the endogenous kinase.

1). We observed that DAH phosphorylation reaches its peak in cellularizing embryos, especially during the slow phase of membrane invagination (Figure 3C, lanes 11–14). The degree of phosphorylation appears to increase during development before cellularization and decreases afterward. These results indicate that DAH phosphorylation is developmentally regulated and may be important for DAH function during cellularization.

A Kinase Activity Is Coimmunoprecipitated with DAH

To understand how the DAH phosphorylation is regulated, we first sought to identify the kinase potentially involved in the phosphorylation. DAH protein was immunoprecipitated, and the immune complex was subjected to in vitro kinase reaction. A series of the phosphorylated species similar to the endogenous DAH species were observed (Figure 4A, lanes 1 and 2; compare Figure 3). These phosphorylated species can also be removed by λ protein phosphatase treatment (our unpublished results). When preimmune serum was used for immunoprecipitation, these phosphorylated species were not detected (Figure 4A, lane 3). A concentration of 1 M NaCl could remove the kinase activities that generated the nonspecific bands in both preimmune and immune complex (lanes 2 and 4), whereas the DAH phosphorylation signals were unaffected in the immune complex (lane 2). Furthermore, DAH phosphorylation was not detected when immunoprecipitation was performed with the use of extracts from *dah*$^-$ mutant embryos (Figure 4C, lanes 1 and 5), indicating that the radiolabeling is specific to the DAH protein.

Because the DAH protein sequence does not contain any kinase domains, it is very likely that a kinase(s) associated with DAH is coimmunoprecipitated. To test this possibility, we washed the kinase activity from the DAH complex and then reconstituted it. First, we tried various reagents to remove the kinase(s) without disrupting the DAH-antibody interaction: 1 M NaCl, 4.5 M NaCl, 1 M KI, 10 mM EGTA, and 10 mM EDTA were used to wash the DAH immune complex extensively before the in vitro kinase reaction. The associated kinase activity is tightly bound in the DAH complex, because it is resistant to high-salt washes up to 4.5 M NaCl, 10 mM EGTA, or 10 mM EDTA (Figure 4B, lanes 8, 9, 11, and 12). However, 1 M KI removes the kinase activity completely (lane 10). To ensure that DAH protein itself was not released upon KI wash, we monitored the amount of the DAH protein by silver stain (lanes 1–6). We detected similar amounts of the DAH protein in all samples, and no significant loss of DAH resulted from the KI wash (lane 4). Furthermore, the lack of DAH phosphorylation is not due to the residual amount of KI left in the DAH complex, which may inhibit the kinase, because the immune complex was washed twice by kinase buffer before the kinase assay and because adding 100 mM KI directly in the kinase reaction did not affect the kinase activity (our unpublished results). These data demonstrate that the DAH-specific kinase activity can be dissociated from DAH by 1 M KI.

In the silver-stained gel, DAH protein appears as a doublet, both bands of which react with DAH antibody by Western blot analysis (our unpublished results) and are missing in extracts from *dah*$^-$ mutant embryos (Figure 4C, lane 1). The presence of a DAH doublet was also described in the previous section (Figure 3A). Treatment of λ phosphatase converted the doublet into a single band that corresponded to the fast-migrating species in the doublet, suggesting that the slower band is a phosphorylated species. Only a minor fraction of the immunoprecipitated DAH is hyperphosphorylated in the in vitro kinase reaction; therefore, hyperphosphorylated DAH is not observed in the silver staining.

Because the kinase activity could be removed from the DAH complex by KI, we tested if we could add the kinase back to reconstitute the DAH phosphorylation reaction. After the DAH immune complex was washed by KI, it was incubated with either immunoprecipitation buffer or the *dah*$^-$ mutant extract (Figure 4C, lanes 7 and 8). The kinase reaction could be reconstituted with the mutant extract (compare lanes 8 and 6), although no DAH protein was immunoprecipitated in the mutant (lanes 1 and 5). Therefore, the kinase activity is independent on DAH protein expression, confirming that DAH has no intrinsic kinase activity.

Examination of the DAH protein sequence reveals the presence of consensus phosphorylation sites for casein kinase (CK) I, CKII, cdc2/cyclin B kinase, glycogen synthase kinase 3, MAPK, cAMP-dependent protein kinase, and PKC. Although the identity of this endogenous DAH kinase(s) remains to be determined, we tested if these potential kinases can phosphorylate DAH in vitro. The DAH immuno-

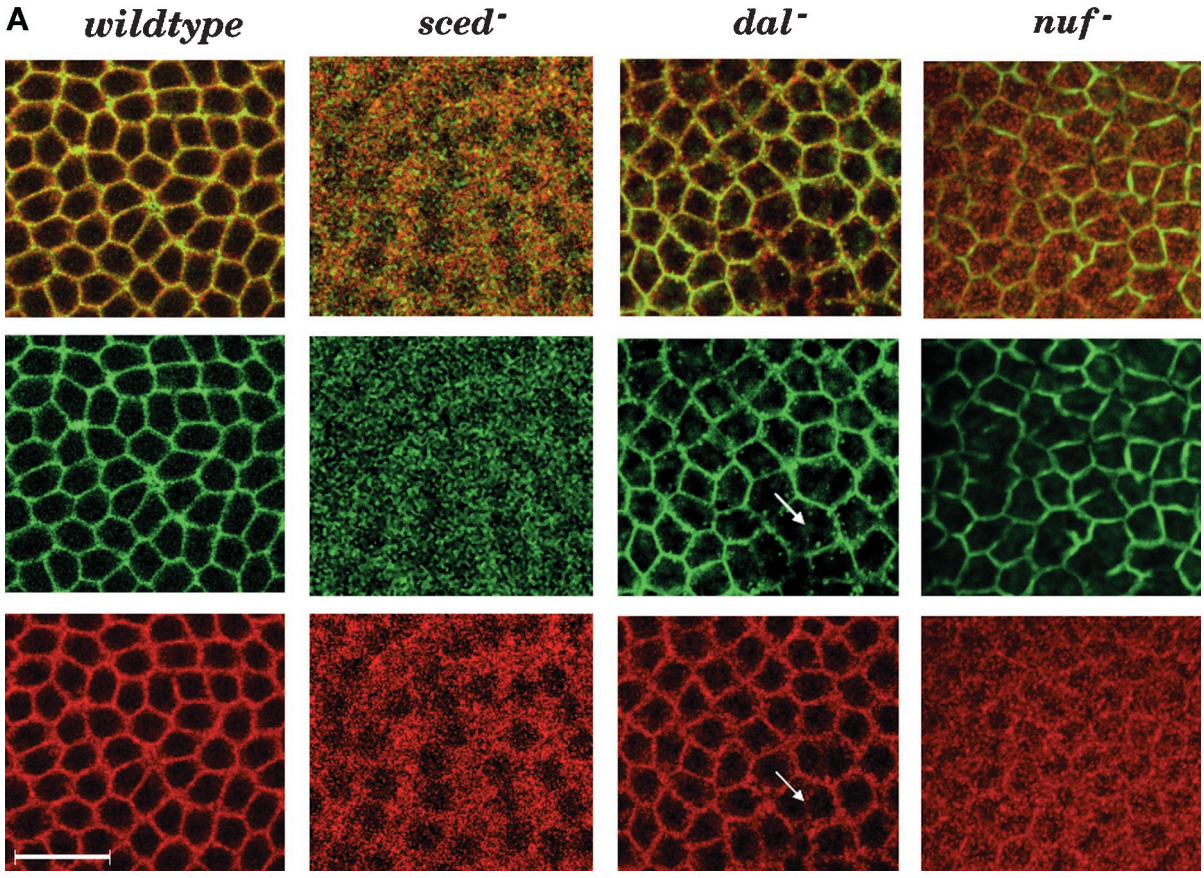

Figure 6.

precipitates were washed by 1 M KI and incubated with these purified kinases, most of which are mammalian proteins (see MATERIALS AND METHODS). Among them, cdc2/cyclin B, CKII, and MAPK do not generate appreciable amounts of DAH phosphorylation (Figure 5, upper panel, lanes 4, 5, and 9). On the other hand, cAMP-dependent protein kinase (PKA), PKC, and glycogen synthase kinase 3 can phosphorylate DAH efficiently. They generate one or two slow-migrating DAH species in the kinase assay (Figure 5, upper panel, lanes 6–8). PKA appears to be very efficient in that it converts all the DAH proteins from the lower band into the upper band of the doublet (lower panel, lane 6). However, it cannot generate more extensive DAH phosphorylation, as shown by the lack of multiple slower-migrating DAH species. In addition, peptide inhibitors for PKA or PKC have no effect on the endogenous kinase activity in the DAH immune complex (our unpublished results), suggesting that PKA and PKC are not involved in DAH phosphorylation. Interestingly, CKI can hyperphosphorylate DAH protein, resulting in a smear of the radiolabeled species with slower electrophoretic mobilities (Figure 5, lane 3). The phosphorylation pattern is similar to the endogenous pattern, except that the exogenous CKI phosphorylates DAH with a much higher efficiency, presumably because purified enzyme is used. Multiple CKI isoforms are present in most organisms, including CKIα and CKIϵ in *Drosophila* (Santos *et al.*, 1996; Kloss *et al.*, 1998). CKI-7, a known CKI inhibitor especially potent for the CKIδ isoform (50% inhibitory concentration = 12 μM) (Chijiwa *et al.*, 1989; Graves *et al.*, 1993; Zhai *et al.*, 1995), has little affect on endogenous kinase activity at the concentration of 10 μM (our unpublished results). Further work will be needed to verify if CKI is the endogenous kinase and, if so, to determine which isoform modifies DAH during embryogenesis.

Interactions between dah and Other Maternal-Effect Genes

To understand the regulation of DAH localization and phosphorylation, we sought to investigate the potential partners with which DAH might interact. Many gene products, besides DAH, participate in the formation and reorganization of the cortical furrows. Maternal-effect mutations such as *grapes* (*grp*), *daughterless-abo-like* (*dal*), *sponge* (*spg*), *scrambled* (*sced*), *waddell* (*wdel*), and *nuclear-fallout* (*nuf*) have been characterized for defective cytoskeletal organization during early embryogenesis (Sullivan *et al.*, 1990, 1993; Postner *et al.*, 1992; Sullivan, personal communication). We are interested in finding possible interactions between DAH and these genes by examining DAH localization and phosphorylation in those mutants.

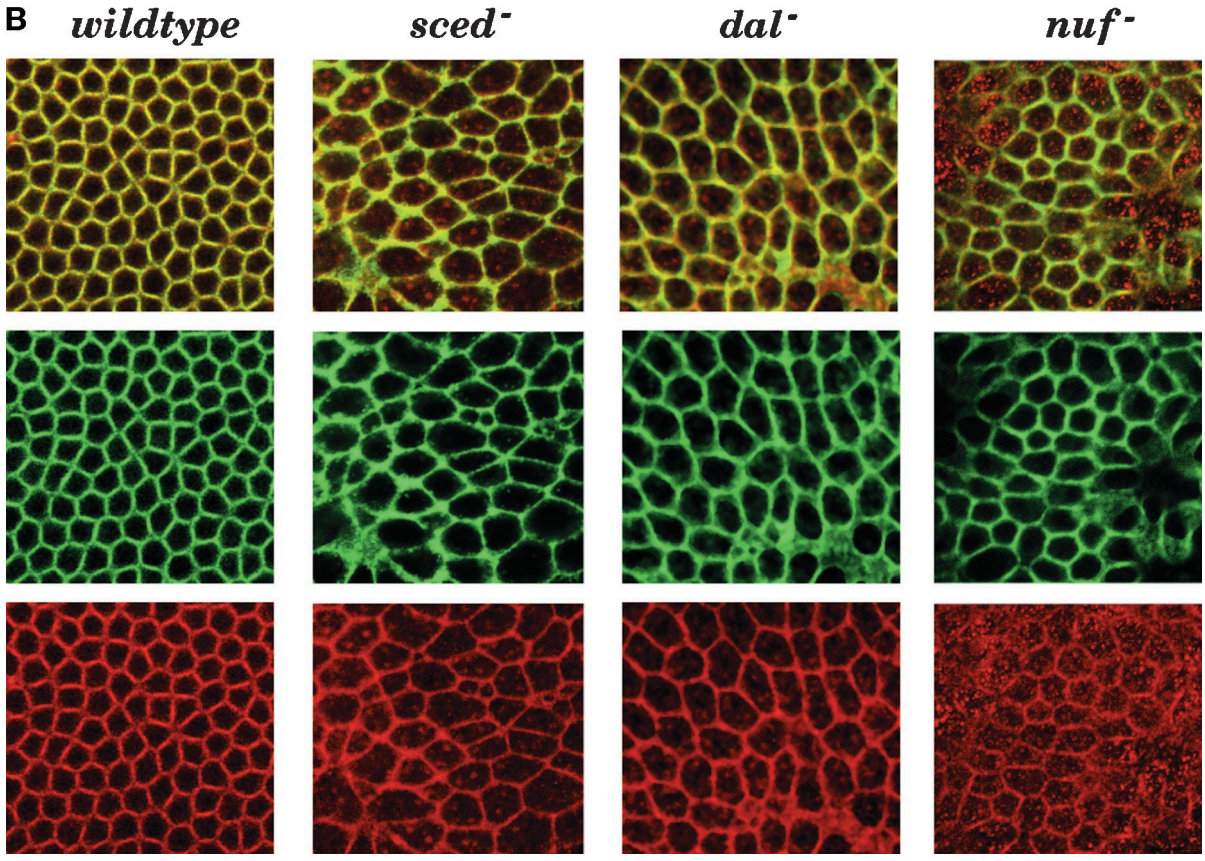

Figure 6 (cont). DAH mislocalizes in *nuf* mutants. (A) Wild-type and mutant embryos (*sced*$^{-}$, *dal*$^{-}$, and *nuf*$^{-}$) in cycle 13 metaphase were double stained with fluorescein-conjugated phalloidin (green channel) and DAH antibody followed by a Cy3-conjugated secondary antibody (red channel). The top panels are the merged images of the green and red channels below them. The arrows point to the disrupted actin network in the *dal* mutant panels. DAH colocalizes with actin in the wild-type embryo (left columns) and in the *sced* and *dal* mutants (middle columns). However, DAH staining is largely diffused in the *nuf* mutant, although incomplete actin hexagons are present (right columns). Bar, 25 μm. (B) Wild-type and mutant embryos in cellularization were prepared as in A. In the wild-type embryo, DAH concentrates in the cleavage furrows (left columns). It localizes to the cleavage furrows in the *sced* and *dal* mutants (middle columns), whereas the DAH localization in *nuf* remains defective (right columns).

During the cortical nuclear divisions (cycles 10–13), actin filaments move from caps above each nucleus into the metaphase furrows at prophase and metaphase, providing a physical barrier for the separation of each mitotic apparatus. *scrambled* and *sponge* mutations both cause almost complete failure in metaphase furrow formation. Although the *scrambled* mutant has normal actin cap formation, the *sponge* mutant lacks actin cap structures (Postner *et al.*, 1992; Sullivan *et al.*, 1993). When mitosis starts in these two mutants, the actin filaments are diffuse in the cytoplasm instead of concentrating in furrow structures. Because DAH normally colocalizes with actin in the metaphase furrows in wild-type embryos (Zhang *et al.*, 1996) (Figure 6A), we are interested in determining where DAH localizes in the absence of the actin networks. In the wild-type embryo at the cycle 13 metaphase, actin (Figure 6A, green channel) and DAH (red channel) are both in metaphase furrows, forming a regular hexagonal array. When we examined the DAH localization in the *sced* mutant, DAH protein showed a diffuse distribution in the cortex similar to the actin distribution (Figure 6A). DAH was excluded from the mitotic spindles and showed no specific localization in the cytoplasm. A similar observation was made in the *spg* mutant as well (our unpublished results). Therefore, in the maternal-effect mutants in which actin-based metaphase furrows are disrupted, the DAH distribution is also affected.

Mutations in *daughterless-abo-like*, *grapes*, *nuclear-fallout*, and *waddell* all result in incomplete metaphase furrows (Sullivan *et al.*, 1990, 1993; Sullivan, personal communication). DAH colocalizes with the defective actin networks in the *dal* mutant (Figure 6A). Although there are disruptions in parts of the furrows where actin is absent (Figure 6A, arrows), DAH shows a diffuse distribution between mitotic spindles. Similar data have been obtained from *grp* and *wdel* mutants as well (our unpublished results). In an interesting contrast, DAH does not localize properly to furrows in the *nuf* mutant (Rothwell *et al.*, 1999) (Figure 6A). Although the overall furrow structure in this *nuf*-derived embryo is not more disrupted than that of the *dal* mutant, DAH shows a diffuse distribution throughout the cortex, whereas actin filaments

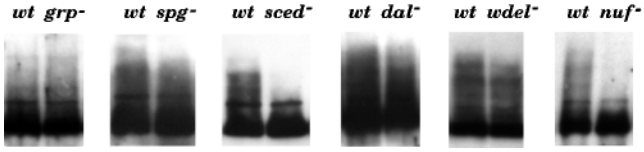

Figure 7. DAH phosphorylation is affected in some of the maternal-effect mutants. Wild-type (*wt*) and mutant embryos (grp^-, spg^-, $sced^-$, dal^-, $wdel^-$, and nuf^-) in the same stages were subjected to single-embryo Western analysis by the DAH antibody. DAH phosphorylation is reduced in the *sced* and *nuf* mutants.

are mostly concentrated in furrows. These results suggest that *nuf* is required for DAH localization to the metaphase furrows.

Our earlier results demonstrated that DAH plays a critical role in the cellularization process. The maternal-effect genes, including *daughterless-abo-like*, *sponge*, and *scrambled*, seem to be dispensable for the cellularization process, because the cleavage furrows form almost normally in these mutants (Sullivan *et al.*, 1990, 1993; Postner *et al.*, 1992). Therefore, we do not anticipate any mislocalization of DAH in these mutants. Indeed, DAH localizes to the cleavage furrows normally in *sced*, *dal* (Figure 6B), and *spg* mutants (our unpublished results). *grapes*, the *Drosophila* homologue of the yeast *checkpoint 1* gene, seems to be critical for turning on the zygotic program, because the *grp* mutant never enters cycle 14 (Fogarty *et al.*, 1997; Sibon *et al.*, 1997). Therefore, we did not include the *grp* mutant in this study. Mutations in *nuclear-fallout*, *waddell*, and *dah* all cause defects in metaphase furrows and cleavage furrows, suggesting that these genes are involved in the formation of both furrows (Sullivan *et al.*, 1993; Zhang *et al.*, 1996; Sullivan, personal communication). Therefore, we investigated if DAH localizes correctly in these two mutants. DAH localizes to the disorganized cleavage furrows in the *wdel* mutant (our unpublished results). However, in the *nuf* mutant, most of the DAH protein is distributed over the entire cortex, although some localizes to parts of the furrows (Figure 6B). It seems that the NUF protein is important for DAH localization not only in the metaphase furrows but also in the cleavage furrows. In all the maternal-effect mutants we examined, we have not observed correct DAH localization in regions where the actin network is disrupted or missing (Figure 6, A and B). This finding suggests that DAH localization/recruitment to the cortical furrows depends on actin networks.

To understand if these maternal-effect genes may regulate DAH expression and its phosphorylation, we performed single-embryo Western analysis on extracts from these mutant embryos. The levels of DAH protein expression in all these mutants are comparable to those in the wild type (Figure 7), suggesting that these maternal-effect genes do not regulate DAH expression. Furthermore, the extent of the DAH phosphorylation is also normal in the *grapes*, *sponge*, *daughterless-abo-like*, and *waddell* mutants, whereas the phosphorylation is greatly reduced in the *nuclear-fallout* and *scrambled* mutations (Figure 7). These results suggest that *nuclear-fallout* and *scrambled* are both involved in the regulation of DAH phosphorylation.

DISCUSSION

DAH is essential for cortical furrow formation during *Drosophila* embryogenesis (Zhang *et al.*, 1996). It is recruited to the invaginating membranes and plays a critical role in furrow extension (Rothwell *et al.*, 1999). To understand DAH function at the molecular level, we investigated the nature of DAH association with membranes. We have shown by biochemical analysis that DAH protein is tightly associated with membranes. The apparent lack of a transmembrane domain sequence in DAH and our failure to detect any carbohydrate and lipid modification suggest that DAH may interact with integral membrane proteins. On the other hand, a fraction of DAH, along with actin, remains insoluble after repeated NP-40 washes, suggesting that DAH may be a component of the cytoskeletal matrix. These observations show that, in addition to the sequence similarity, DAH protein shares some common features with the carboxyl terminus of dystrophin. The carboxyl terminus anchors dystrophin to the plasma membrane through its interaction with transmembrane glycoproteins that bind laminin in muscle cells (reviewed by Ervasti and Campbell, 1993). It enables dystrophin to link the actin cytoskeleton to the extracellular matrix with a direct interaction between actin filaments and the amino terminus of dystrophin. Because DAH is also tightly associated with membranes, it is possible that DAH mediates or stabilizes the linkage of the actin cytoskeleton to membranes in early embryos.

This model is also supported by the immunofluorescence analysis performed by Rothwell *et al.* (1999). DAH has been found on the membrane-containing particles, marked by anti-phosphotyrosine antibody. More interestingly, particles of actin filaments lie side by side and appear to be attached to the DAH particles. These localization data suggest that DAH may associate with both membranes and the actin cytoskeleton. Those particles accumulate during the interphase of the cell cycle and seem to fuse with invaginating membrane furrows during mitosis. It is likely that those particles are required for furrow extension and that DAH is involved in delivering membrane vesicles and the actin cytoskeleton to the furrows where membranes invaginate. Alternatively, DAH may play a role in stabilizing the interactions between the actin cytoskeleton and membrane vesicles at the cleavage furrows.

At least six phosphorylated species exist in vivo, and the phosphorylation reaches its peak at a stage at which DAH function is critical for embryogenesis. These results suggest that DAH phosphorylation might be functionally relevant. To identify the possible kinase involved in DAH phosphorylation, we examined the in vitro phosphorylation in the DAH immunoprecipitate. We found a kinase activity in the DAH immune complex that can hyperphosphorylate DAH protein in vitro. A potential candidate for the DAH kinase is CKI. Exogenous CKI can efficiently hyperphosphorylate DAH protein in the immune complex. Two CKI isoforms, α and ϵ, have been found in *Drosophila* (Santos *et al.*, 1996; Kloss *et al.*, 1998). CKIα is specifically expressed in early embryos and adult females, suggesting a maternal function of this CKI isoform. It is activated by γ-irradiation and may be involved in the DNA repair pathway. CKIϵ is encoded by the *Drosophila* clock gene *double-time*. It regulates the phosphorylation state of PER protein and controls circadian rhythms in fly. YCK2, a CKI isoform in *Saccharomyces cerevi-*

siae, is tightly associated with the plasma membrane and localizes to sites of polarized growth and cytokinesis (Vancura *et al.*, 1994; Robinson *et al.*, 1999). It is required for accurate bud site selection and proper septin organization. Therefore, it would be interesting to determine if any isoform of *Drosophila* CKI is also involved in the cytoskeletal organization and in DAH phosphorylation.

Several maternal-effect genes have been shown to function in the organization and rearrangement of actin networks in early embryos. It would be interesting to determine if *dah* functions in the same pathway as these genes. We have shown that the recruitment of DAH to the cortical furrows is unaffected in the *scrambled*, *sponge*, *daughterless-abo-like*, *grapes*, and *waddell* mutants, suggesting that these genes may not be directly involved in DAH function. However, DAH recruitment is greatly reduced in the *nuclear-fallout* mutant. We have demonstrated that, in addition to the mislocalization of DAH in the metaphase furrows, as shown earlier by Rothwell *et al.* (1999), DAH is also largely mislocalized in the cleavage furrows. Therefore, NUF, a centrosomal protein, seems to play critical roles in recruiting important components, such as DAH and actin, to the cortical furrows.

DAH protein phosphorylation is significantly reduced in two maternal-effect mutants, *nuclear-fallout* and *scrambled*. A potential role of phosphorylation is to regulate the interactions of DAH with membrane protein and/or actin-binding protein. Thus, DAH phosphorylation could facilitate the recruitment of the DAH particles that contain lipid components and actin cytoskeleton to the cortical furrows. Importantly, DAH phosphorylation reaches its peak at a stage at which the membrane synthesis is most demanding during early embryogenesis. In the *nuf* mutant, hypophosphorylated DAH protein fails to localize to the metaphase furrows and is found only in a subset of the defective cleavage furrows. This failure of DAH recruitment could be a direct result of deficient phosphorylation. In the *sced* mutant, although hypophosphorylated DAH localizes to the cleavage furrows, there are greatly reduced furrow structures in these embryos. Cellularization occurs only at the pole regions of the *sced* embryos, and the actin networks appear thinner and abnormal compared with those in the wild type (Postner *et al.*, 1992; Sullivan *et al.*, 1993) (Figure 6B). Therefore, it is possible that, despite a reduced efficiency of particle recruitment as a result of hypophosphorylation, a fraction of DAH could still be recruited into the remaining actin cytoskeleton. It will be of great interest to determine the functions of DAH phosphorylation during development.

ACKNOWLEDGMENTS

We are indebted to the following colleagues for the generous gifts used in our experiments: W. Theurkauf, C. Nuesslein-Volhard, Y. Shi, and P. Blackshear. The use of confocal fluorescence microscope facilities at the Duke Comprehensive Cancer Center and in Vann Bennett's laboratory is gratefully appreciated. This work was supported in part by National Institutes of Health grant GM29006.

REFERENCES

Baumgartner, S., Littleton, J.T., Broadie, K., Bhat, M.A., Harbecke, R., Lengyel, J.A., Chiquet-Ehrismann, R., Prokop, A., and Bellen, H.J. (1996). A *Drosophila* neurexin is required for septate junction and blood-nerve barrier formation and function. Cell *87*, 1059–1068.

Bordier, C. (1981). Phase separation of integral membrane proteins in Triton X-114 solution. J. Biol. Chem. *256*, 1604–1607.

Chijiwa, T., Hagiwara, M., and Hidaka, H. (1989). A newly synthesized selective casein kinase I inhibitor, *N*-(2-aminoethyl)-5-chloroisoquinoline-8-sulfonamide, and affinity purification of casein kinase I from bovine testis. J. Biol. Chem. *264*, 4924–4927.

Ervasti, J.M., and Campbell, K.P. (1993). Dystrophin and the membrane skeleton. Curr. Opin. Cell Biol. *5*, 82–87.

Foe, V.E., and Alberts, B.M. (1983). Studies of nuclear and cytoplasmic behavior during the five mitotic cycles that precede gastrulation in *Drosophila* embryogenesis. J. Cell Sci. *61*, 31–70.

Fogarty, P., Campbell, S.D., Abu-Shumays, R., Phalle, B.S., Yu, K.R., Uy, G.L., Goldberg, M.L., and Sullivan, W. (1997). The *Drosophila* grapes gene is related to checkpoint gene chk1/rad27 and is required for late syncytial division fidelity. Curr. Biol. *7*, 418–426.

Fyrberg, E.A., and Goldstein, L.S. (1990). The *Drosophila* cytoskeleton. Annu. Rev. Cell Biol. *6*, 559–596.

Geiger, B. (1983). Membrane-cytoskeleton interaction. Biochim. Biophys. Acta *737*, 305–341.

Graff, J.M., Rajan, R.R., Randall, R.R., Nairn, A.C., and Blackshear, P.J. (1991). Protein kinase C substrate and inhibitor characteristics of peptides derived from the myristoylated alanine-rich C kinase substrate (MARCKS) protein phosphorylation site domain. J. Biol. Chem. *266*, 14390–14398.

Graves, P.R., Haas, D.W., Hagedorn, C.H., DePaoli-Roach, A.A., and Roach, P.J. (1993). Molecular cloning, expression, and characterization of a 49-kilodalton casein kinase I isoform from rat testis. J. Biol. Chem. *268*, 6394–6401.

Graziani, G., Ron, D., Eva, A., and Srivastava, S.K. (1989). The human *dbl-proto-oncogene* product is a cytoplasmic phosphoprotein which is associated with the cytoskeletal matrix. Oncogene *4*, 823–829.

Hortsch, M. (1994). Preparation and analysis of membranes and membrane proteins from *Drosophila*. Methods Cell Biol. *44*, 289–301.

Karr, T.L., and Alberts, B.M. (1986). Organization of the cytoskeleton in early *Drosophila* embryos. J. Cell Biol. *102*, 1494–1509.

Kellogg, D.R., Mitchison, T.J., and Alberts, B.M. (1988). Behavior of microtubules and actin filaments in living *Drosophila* embryos. Development *103*, 675–686.

Kloss, B., Price, J.L., Saez, L., Blau, J., Rothenfluh, A., Wesley, C.S., and Young, M.W. (1998). The *Drosophila* clock gene double-time encodes a protein closely related to human casein kinase Iepsilon. Cell *94*, 97–107.

Lee, M.P., Brown, S.D., Chen, A., and Hsieh, T.S. (1993). DNA topoisomerase I is essential in *Drosophila melanogaster*. Proc. Natl. Acad. Sci. USA *90*, 6656–6660.

Magee, A.I., Koyama, A.H., Malfer, C., Wen, D., and Schlesinger, M.J. (1984). Release of fatty acids from virus glycoproteins by hydroxylamine. Biochim. Biophys. Acta *798*, 156–166.

Maley, F., Trimble, R.B., Tarentino, A.L., and Plummer, T.H., Jr. (1989). Characterization of glycoproteins and their associated oligosaccharides through the use of endoglycosidases. Anal. Biochem. *180*, 195–204.

McAlister, L., and Holland, M.J. (1985). Differential expression of the three yeast glyceraldehyde-3-phosphate dehydrogenase genes. J. Biol. Chem. *260*, 15019–15027.

McCrea, P.D., and Gumbiner, B.M. (1991). Purification of a 92-kDa cytoplasmic protein tightly associated with the cell-cell adhesion molecule E-cadherin (uvomorulin): characterization and extractability of the protein complex from the cell cytostructure. J. Biol. Chem. *266*, 4514–4520.

Merrill, P.T., Sweeton, D., and Wieschaus, E. (1988). Requirements for autosomal gene activity during precellular stages of *Drosophila melanogaster*. Development *104*, 495–509.

Nagafuchi, A., and Takeichi, M. (1988). Cell binding function of E-cadherin is regulated by the cytoplasmic domain. EMBO J. *7*, 3679–3684.

Postner, M.A., Miller, K.G., and Wieschaus, E.F. (1992). Maternal effect mutations of the *sponge* locus affect actin cytoskeletal rearrangements in *Drosophila melanogaster* embryos. J. Cell Biol. *119*, 1205–1218.

Rabinowitz, M. (1941). Studies on the cytology and early embryology of the egg of *Drosophila melanogaster*. J. Morphol. *69*, 1–49.

Robinson, L.C., Bradley, C., Bryan, J.D., Jerome, A., Kweon, Y., and Panek, H.R. (1999). The Yck2 yeast casein kinase 1 isoform shows cell cycle–specific localization to sites of polarized growth and is required for proper septin organization. Mol. Biol. Cell *10*, 1077–1092.

Rothwell, W.F., Fogarty, P., Field, C.M., and Sullivan, W. (1998). Nuclear-fallout, a *Drosophila* protein that cycles from the cytoplasm to the centrosomes, regulates cortical microfilament organization. Development *125*, 1295–1303.

Rothwell, W.F., Zhang, C.X., Zelano, C., Hsieh, T.-s., and Sullivan, W. (1999). The *Drosophila* centrosomal protein Nuf is required for recruiting Dah, a membrane associated protein, to furrows in the early embryo. J. Cell Sci. *112*, 2885–2893.

Santos, J.A., Logarinho, E., Tapia, C., Allende, C.C., Allende, J.E., and Sunkel, C.E. (1996). The casein kinase 1 alpha gene of *Drosophila melanogaster* is developmentally regulated and the kinase activity of the protein induced by DNA damage. J. Cell Sci. *109*, 1847–1856.

Schejter, E.D., Rose, L.S., Postner, M.A., and Wieschaus, E. (1992). Role of the zygotic genome in the restructuring of the actin cytoskeleton at the cycle-14 transition during *Drosophila* embryogenesis. Cold Spring Harbor Symp. Quant. Biol. *57*, 653–659.

Schejter, E.D., and Wieschaus, E. (1993). Functional elements of the cytoskeleton in the early *Drosophila* embryo. Annu. Rev. Cell Biol. *9*, 67–99.

Sibon, O.C., Stevenson, V.A., and Theurkauf, W.E. (1997). DNA-replication checkpoint control at the *Drosophila* midblastula transition. Nature *388*, 93–97.

Strand, D., Raska, I., and Mechler, B.M. (1994). The *Drosophila* lethal(2)giant larvae tumor suppressor protein is a component of the cytoskeleton. J. Cell Biol. *127*, 1345–1360.

Sullivan, W., Fogarty, P., and Theurkauf, W. (1993). Mutations affecting the cytoskeletal organization of syncytial *Drosophila* embryos. Development *118*, 1245–1254.

Sullivan, W., Minden, J.S., and Alberts, B.M. (1990). *daughterless-abo-like*, a *Drosophila* maternal-effect mutation that exhibits abnormal centrosome separation during the late blastoderm divisions. Development *110*, 311–323.

Vancura, A., Sessler, A., Leichus, B., and Kuret, J. (1994). A prenylation motif is required for plasma membrane localization and biochemical function of casein kinase I in budding yeast. J. Biol. Chem. *269*, 19271–19278.

Ward, R.E., Lamb, R.S., and Fehon, R.G. (1998). A conserved functional domain of *Drosophila* coracle is required for localization at the septate junction and has membrane-organizing activity. J. Cell Biol. *140*, 1463–1473.

Wieschaus, E., and Sweeton, D. (1988). Requirements for X-linked zygotic gene activity during cellularization of early *Drosophila* embryos. Development *104*, 483–493.

Zhai, L., Graves, P.R., Robinson, L.C., Italiano, M., Culbertson, M.R., Rowles, J., Cobb, M.H., DePaoli-Roach, A.A., and Roach, P.J. (1995). Casein kinase I gamma subfamily: molecular cloning, expression, and characterization of three mammalian isoforms and complementation of defects in the *Saccharomyces cerevisiae* YCK genes. J. Biol. Chem. *270*, 12717–12724.

Zhang, C.X., Lee, M.P., Chen, A.D., Brown, S.D., and Hsieh, T. (1996). Isolation and characterization of a *Drosophila* gene essential for early embryonic development and formation of cortical cleavage furrows. J. Cell Biol. *134*, 923–934.